Sensitivity analysis of plunger-type wavemakers with water current

Stephanie Lowell
Department of Mechanical and Aerospace Engineering
Carleton University
Ottawa, Canada
stephanie.lowell@carleton.ca

Rishad A. Irani
Department of Mechanical and Aerospace Engineering
Carleton University
Ottawa, Canada
rishad.irani@carleton.ca

***Abstract*—The inclusion of current in a water channel is a critical requirement for recreating accurately scaled ocean environments in a laboratory. In this paper, the effect of a uniform current on the theoretical model of a plunger-type wavemaker has been investigated through a variance-based global sensitivity analysis. The output of the wavemaker model is represented by the ratio of wave amplitude to stroke amplitude. Therefore, the sensitivity analysis evaluates the influence of all uncertain input parameters on the output variance of the model. In addition to the water current, the uncertain input parameters for the wavemaker model were established as the wave frequency, wedge angle, mean wedge depth, water height, and node points on the wavemaker boundary. To account for a range of limitations for both the plunger and the water channel in which it oscillates, the sensitivity analysis was performed for a broad distribution of each parameter.**

The analysis determined that the wave frequency had the highest influence on the output variance of the wavemaker model. For a uniform water current, the first order and total effect sensitivity indices were estimated as $0.74 \pm 0.30\%$ and $6.84 \pm 0.16\%$, respectively. Although the sensitivity of the model to the current was relatively low compared to the wave frequency, there exists an impact due to the interaction of the current with the other parameters. Therefore, it was established that the inclusion of the current in the plunger-type wavemaker model is essential for application of the model to an experimental setup.

***Index Terms*—Wavemakers, Plunger-type, Water current, Global sensitivity analysis, sensitivity indices**

I. Introduction

Wavemakers are a convenient method for generating and observing water waves in a controlled laboratory setting. The three most common types of wavemakers used in test tanks are piston-type, flap-type, and plunger-type wavemakers [1]. Of the existing wavemakers, plunger-types are the only wavemakers that allow for water flow across its boundary; however, research with the plunger system has focused on water without a steady current.

The general theory for waves produced on a water surface by a generator was initially established by Havelock [2] and commonly referred to as "wavemaker theory". The specific application of wavemaker theory to a wedge-shaped wavemaker was established by Wang [3] who showed that the ratio of the water wave amplitude to the plunger stroke amplitude will be dependent on the wavenumber and the mean width of the wedge at the still water level. By using the boundary collocation method, Wu [4] developed a semi-analytical method to study waves generated by a plunger-type wavemaker that demonstrated the required inclusion of water height in the wavemaker model. The wave profiles produced by a plunger-type wavemaker were studied by Ellix and Arumugam [5] which Wu [4], [6] referenced for comparison to the theoretical model; however, both theory and experiment were only applied to the still water case and did not include the effect of a steady current. The plunger-type wavemaker theory was advanced by McPhee [7], who proposed that the uniform current in a flume tank be taken into account, but experimental validation was outside the scope of the study.

For the size of the wedge and geometry of the flume tank at Carleton University, the new theoretical plunger-type wavemaker model [7] predicts that the ratio between the wave amplitude and the stroke amplitude of the plunger for a zero velocity current will be equal to 0.62 for a wave frequency of 3.2π rad/s. Using the standard theory, which does not incorporate the influence of current, the ratio would remain constant for any value of water current. However, experimental measurements indicate a 25.6% average decrease in the ratio of the wave amplitude to stroke amplitude as the current velocity increases from 0.000 m/s to 0.305 m/s. Over the same range in current, the new wavemaker model which accounts for the flow, theorizes a 20.3% decrease in the amplitude ratio. Therefore, the experimental results indicate that there is an influence due to current on the wavemaker model output.

The scope of the current paper aims to investigate the influence of water current on the theoretical plunger-type wavemaker model through a variance-based global sensitivity analysis (GSA). The theoretical development of the GSA is well established [8], and while it has been applied to a variety of scientific models, to the authors' knowledge there has been no sensitivity analysis conducted on the plunger-type wavemaker model. As a result, the impact and understanding of water current on the design and operation of a plunger-type wavemaker is an essential contribution to the field. The present study seeks to provide insight to the input parameters of the theoretical plunger-type wavemaker model, with a focus on how the inclusion of water current impacts the output of the model and how the current parameter interacts with other uncertain input parameters. The global sensitivity analysis will

978-1-7281-5446-6/20/$31.00 ©2020 IEEE

provide understanding towards the strengths and weaknesses of the wavemaker model and a basis for the design of future plunger-type wavemakers.

Section II of this paper provides an overview of the plunger-type wavemaker theoretical model. Section III outlines the theory of global sensitivity analysis including validation of the code using the Ishigami function (Section III-A). Section IV provides the results and discussion of the sensitivity analysis of the plunger-type wavemaker model for a general distribution of each uncertain input parameter. The paper is concluded in Section V with a summary of the findings and applications.

II. Plunger-type Wavemaker Model

A schematic of the plunger-type wavemaker problem for a wedge with a triangular cross-section in a laboratory water channel is displayed in Fig. 1, where x represents the horizontal axis and z is the vertical axis. The angle β is measured

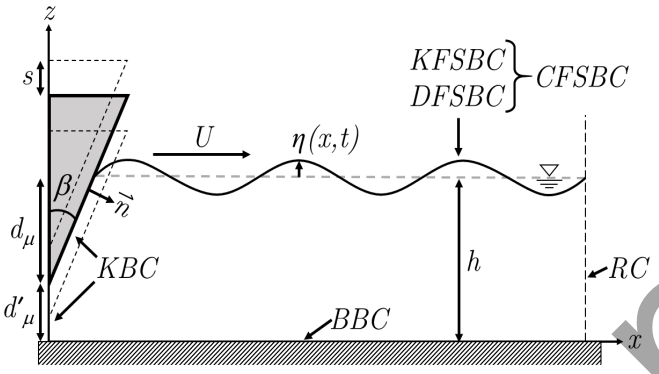

Figure 1. Schematic of an plunger-type wavemaker in a laboratory water channel with current U. The channel is defined by four conditions. The far-field radiation condition (RC), bottom boundary condition (BBC), kinematic boundary condition (KBC), and combined free surface boundary condition (CFSBC) which includes the kinematic free surface boundary condition (KFSBC) and dynamic free surface boundary condition (DFSBC).

between the vertical z axis and the hypotenuse of the wedge, while the mean wedge depth d_μ is measured at the still water height h. The clearance between the bottom of the water channel and the wedge is denoted d'_μ and $\vec{n}$ represents the vector normal to the surface of the wedge. The position of the free surface of the water is represented by $\eta(x,t)$ at position x and time t relative to the plane $z = h$. Forward waves are produced by the vertical displacement s of the plunger as it oscillates in the water column. Thus, the water wave length and height are controlled by the oscillation frequency and fluid displacement of the plunger. The oscillating motion allows for flow across the lateral boundary throughout the duration of the operation. The magnitude of the water current U is positive along the x-axis when moving the same direction as the waves produced by the wavemaker. The water channel in Fig. 1 can be defined by four boundary conditions and a radiation condition (RC) that ensures only the existance of progressive waves at large distance from the plunger [4]. The bottom boundary condition (BBC) describes the horizontal plane along $z = 0$ where the no flow condition applies. The combined free surface boundary condition (CFSBC) describes the free surface of the water which includes the kinematic free surface boundary condition (KFSBC) and the dynamic free surface boundary condition (DFSBC). The KFSBC ensures that there is no flow across the free surface from the water to the air, while the DFSBC constrains a uniform pressure distribution across the free surface boundary. The final boundary condition is a kinematic boundary condition (KBC) that exists along the inclined surface of the plunger wedge and the clearance defined by d'_μ.

The transfer function between the wave amplitude a and the stroke amplitude of the plunger s provides an important metric for wavemaker design. For a known stroke amplitude, the wave amplitude can be determined by examining the water wave profile $\eta(x,t)$ produced by the wavemaker. Under the assumption of classic hydrodynamics, the fluid flow is inviscid, incompressible, and irrotational. Thus, the problem can be defined by small amplitude gravity wave theory where there exists a velocity potential ϕ that satisfies the continuity equation,

$$\nabla \cdot \nabla \phi = 0, \tag{1}$$

where the gradient ∇ leads to the Laplace equation. Solving for the linear wave profile therefore becomes a boundary value problem constrained by the four boundary conditions and radiation condition shown in Fig. 1. The BBC at $z = 0$ is mathematically defined by,

$$\left(\frac{\partial \phi}{\partial z}\right)_{z=0} = 0. \tag{2}$$

Similarly, the CFSBC at $z = h$ is expressed by,

$$\left(\frac{\partial \phi}{\partial z} - \frac{\omega^2}{g}\phi\right)_{z=h} = 0, \tag{3}$$

where ω is the wave frequency and g is the acceleration due to gravity, equal to 9.81 m/s^2. Assuming no leakage around the wedge, the KBC along the wavemaker and the clearance section is respectively defined by,

$$\left(\frac{\partial \phi}{\partial n}\right)_{d'_\mu \le z \le h} = s\omega \sin(\beta)\cos(\omega t), \tag{4a}$$

$$\left(\frac{\partial \phi}{\partial x}\right)_{0 \le z < d'_\mu} = 0. \tag{4b}$$

When $\beta = 0$, the condition in (4a) is equal to that of (4b); therefore, a single equation can be used to describe the KBC for $\beta \ge 0$ and $0 < z < h$. Combining (4a) and (4b), the modified KBC on the wavemaker at $x = (z - d'_\mu)\tan(\beta)$ is expressed as,

$$\frac{\partial \phi}{\partial x} - \frac{\partial \phi}{\partial z}\tan(\beta) = s\omega \tan(\beta)\cos(\omega t). \tag{5}$$

One form of the velocity potential $\phi(x,z)$ which solves the Laplace equation and also satisfies the BBC, CFSBC, and RC is given by,

$$\phi(x,z) = A_0 \cosh(k_p z) e^{i_m k_p x} + \sum_{n=1}^{\infty} A_n \cos(k_n z) e^{-k_n x}, \tag{6}$$

where $n = 1, 2, \ldots, \infty$, i_m is the imaginary number, A_0 and A_n are unknown coefficients of the velocity potential whose values are to be determined, and the wavenumbers k_p and k_n represent progressive and standing waves, respectively [4]. Equation (6) is constrained by the dispersion relationship of both wavenumbers k_p and k_n defined by,

$$\omega^2 = g k_p \tanh(k_p h), \tag{7}$$

$$\omega^2 = -g k_n \tanh(k_n h). \tag{8}$$

For the no current condition, the dispersion relations in (7) and (8) hold true; however, water waves in a uniform current U experience a Doppler shift. Therefore, as initially proposed by McPhee [7], the dispersion relation used to constrain the velocity potential for the plunger-type wavemaker boundary value problem must be modified to account for the current velocity U. By shifting the frequency ω, the modified dispersion relation for the progressive wavenumber k_p can be expressed as,

$$(\omega - k_p U)^2 = g k_p \tanh(k_p h). \tag{9}$$

From the definition of phase velocity where the celerity C is equal to ω/k_p, (9) can be rewritten as,

$$(C - U)^2 = \frac{g}{k_p} \tanh(k_p h). \tag{10}$$

The solution to (10) in terms of C is determined using the quadratic solution and replacing the wavenumber k_p with ω/C [9], such that,

$$C = \left(U + \frac{g}{2\omega}\right) + \sqrt{\frac{Ug}{\omega} + \frac{1}{4}\left(\frac{g}{\omega}\right)^2}. \tag{11}$$

For convenience, a reference frame that moves with the current is adopted such that the solution to the boundary value problem in the no current condition can still be used. To relate the moving reference frame to the stationary frame, the wavelength must be equal in both systems; therefore the period T' relative to the moving frame relates to the period T in the stationary frame by,

$$T' = \frac{T}{(1 - \frac{U}{C})}. \tag{12}$$

By describing the period, and hence the frequency, by (12), the current $U \geq 0$ is taken into consideration for the wavemaker boundary value problem.

With the dispersion constraint modified to include the effect of current, substituting the velocity potential solution defined by (6) into the modified KBC expressed in (5) yields an expression from which A_0 and A_n can be determined,

$$\begin{aligned}
&\Bigg[i_m A_0 k_p \cosh(k_p z) e^{i_m k_p (z - d'_\mu)\tan(\beta)} - \\
&\quad \sum_{n=1}^{\infty} A_n k_n \cos(k_n z) e^{-k_n (z - d'_\mu)\tan(\beta)} \Bigg] - \\
&\quad \Bigg[A_0 k_p \sinh(k_p z) e^{i_m k_p (z - d'_\mu)\tan(\beta)} - \\
&\quad\quad \sum_{n=1}^{\infty} A_n k_n \sin(k_n z) e^{-k_n (z - d'_\mu)\tan(\beta)} \Bigg] \tan(\beta) \\
&\quad\quad = s\omega \tan(\beta).
\end{aligned} \tag{13}$$

To solve for the coefficients A_0 and A_n, a semi-analytical solution using the boundary collocation method is applied [4]. For the wavemaker problem, the boundary is defined as the KBC in Fig. 1 which includes the inclined surface of the wedge and the clearance between wedge bottom and channel bottom d'_μ. The boundary is divided into segments of equal vertical length with two node points at each end of a segment totalling M node points. To satisfy (13) at all M node points, it is expressed in matrix form as,

$$\mathbf{B}\mathbf{A}' = \mathbf{D}, \tag{14}$$

where $\mathbf{B}$ is a mxn matrix, $\mathbf{A}'$ is a nx1 matrix, and $\mathbf{D}$ is a mx1 matrix with the number of node points M representing the number of matrix rows m and total number of waves n representing the number of matrix columns. The elements of matrices $\mathbf{B}$, $\mathbf{A}'$, and $\mathbf{D}$ are expressed as,

$$\begin{aligned}
B_{m1} = k_p h \Bigg(& i_m \cosh\left[k_p h \left(\frac{z}{h}\right)_m\right] - \\
& \tan(\beta) \sinh\left[k_p h \left(\frac{z}{h}\right)_m\right] \Bigg) e^{i_m k_p h \tan(\beta)\left(\frac{z - d'_\mu}{h}\right)_m},
\end{aligned} \tag{15}$$

$$\begin{aligned}
B_{mn} = -k_{n-1} h \Bigg(& cos\left[k_{n-1} h \left(\frac{z}{h}\right)_m\right] - \\
& \tan(\beta) \sin\left[k_{n-1} h \left(\frac{z}{h}\right)_m\right] \Bigg) e^{-k_{n-1} h \tan(\beta)\left(\frac{z - d'_\mu}{h}\right)_m}, \\
& n \neq 1,
\end{aligned} \tag{16}$$

$$A'_1 = \frac{A_0}{s\omega h}, \tag{17}$$

$$A'_n = \frac{A_{n-1}}{s\omega h}, \quad n \neq 1, \tag{18}$$

$$D_m = \tan(\beta), \tag{19}$$

where B_{m1} represents a single progressive wave and B_{mn} represents the standing waves. Equation (14) is solved using a least squares method to minimize the sum of quadratic error

by multiplying both sides by the Hermitian transpose of $\mathbf{B}$ denoted $\mathbf{B}^T$ such that,

$$\mathbf{B}^T\mathbf{B}\mathbf{A}' = \mathbf{B}^T\mathbf{D}. \tag{20}$$

Wu [4] suggests using a finite number of waves by setting $n = 16$ such that the approximate solution to (20) includes one progressive wave and 15 standing waves. The RC ensures that the standing waves will decay with distance from the wavemaker such that terms in (6) relating to k_n will be negligible. Thus, taking the real part of the first term in (6), the velocity potential ϕ reduces to,

$$\phi = \mathrm{Re}\big[A_0 \cosh(k_p z) e^{i_m(k_p x - \omega t)}\big]. \tag{21}$$

The linear wave profile of the free surface $\eta(x,t)$ where only the progressive wave exists is expressed as,

$$\eta(x,t) = \frac{1}{g}\frac{\partial \phi}{\partial t} = \mathrm{Re}\Big[\frac{-i_m \omega A_0}{g}\cosh(k_p h) e^{i_m(k_p x - \omega t)}\Big], \tag{22}$$

where the amplitude of the wave a is defined by,

$$a = \left|\frac{-i_m \omega A_0}{g}\cosh(k_p h)\right|. \tag{23}$$

By dividing both sides of (23) by the stroke amplitude s, the theoretical plunger-type wavemaker model which relates the water wave amplitude a to the stroke amplitude s is derived to be,

$$\frac{a}{s} = \left|-i_m A_1' k_p h \mathrm{sinh}(k_p h)\right|, \tag{24}$$

where A_1' is defined by (17). However, since the definition of A_1' is dependent on the unknown coefficient A_0, it is determined by solving (20). Equation (24) is the key output equation for the plunger-type wavemaker model which will be investigated in the GSA.

The wavemaker model is non-linear and requires six input parameters including the water current U. The water current, along with the wave frequency ω, will impact the value of k_p. The progressive wavenumber is also required to determine A_1'; therefore, A_1' will be dependent on U and ω, as well as additional parameters including the water height h, mean wedge depth d_μ, wedge angle β, and the number of node points M used to describe the theoretical KBC. Although (24) has the same form of the wavemaker model as presented by Wu [4], its inclusion of the current causes an effect on the output of the model. Fig. 2 plots the effect of an applied uniform current U flowing in the direction of the propagating wave on the amplitude ratio a/s. The "new model" represents the wavemaker model defined by (24) which includes current, while the "standard model" excludes the influence of current. The remaining input parameters have been fixed where $\omega = 3.2\pi$ rad/s, $\beta = 25.7°$, $d_\mu = 0.12$ m, $h = 0.583$ m, and $M = 200$. Since the standard model does not account for the current velocity, the value of a/s remains constant for all values of U. On the contrary, the new model demonstrates that for a constant stroke amplitude s, the amplitude of the waves a propagating from the wavemaker will be smaller if a steady current is included. As the current velocity is increased, the wave amplitude will further decrease under a constant stroke amplitude. The behaviour of the relationship in Fig. 2 is consistent for the wavemaker model; however, the exact value of a/s will also be dependent on the values of the input parameters that were fixed. Therefore, application of the GSA to the new plunger-type wavemaker model is essential as it will provide an estimated sensitivity measure for the uncertain input parameters which include the current U, wave frequency ω, wedge angle β, mean wedge depth d_μ, water height h, and node points M.

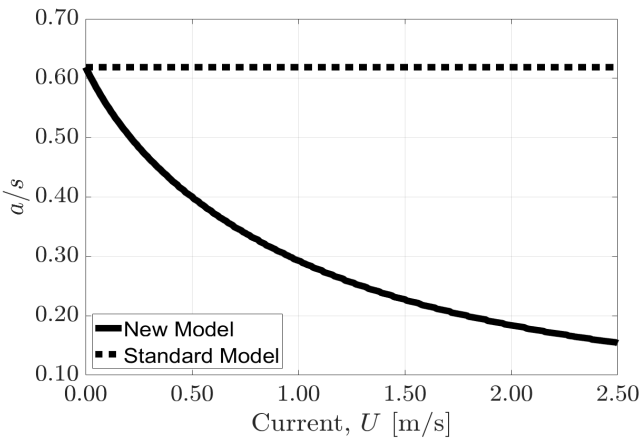

Figure 2. The ratio of the wave amplitude to stroke amplitude for a uniform current as predicted by the new wavemaker model which incorporates U and the standard model which does not include U. The values of the remaining input parameters were fixed at $\omega = 3.2\pi$ rad/s, $\beta = 25.7°$, $d_\mu = 0.12$ m, $h = 0.583$ m, and $M = 200$.

III. Global Sensitivity Analysis Theory

The sensitivity analysis herein aims to quantify the relative importance of the uncertain input parameters for the plunger-type wavemaker model. Compared to a derivative-based, or local, sensitivity analysis, the GSA has the advantage of determining the influence of each individual input parameter on the outcome of the model as well as the degree of interaction between parameters. To allow for the study of the non-linear plunger-type wavemaker model, variance-based methods of sensitivity analyses were used [8]. For these methods, the influence of the input parameters are referred to as sensitivity indices. For the variance-based GSA, the plunger-type wavemaker model described by (24) is represented by the form,

$$Y = f(X_1, X_2, \ldots, X_k), \tag{25}$$

where the output Y is a scalar and X_i represents the model's uncertain input parameters where $i = 1, 2, \ldots, k$. The first order sensitivity index for a given parameter X_i is the ratio of the partial variance V_i taken over X_i to the overall variance of the model V. In the present study, the sensitivity indices were numerically computed using Monte Carlo sampling methods [10].

For the Monte Carlo analysis, $\mathbf{G}$ and $\mathbf{H}$ are two independent matrices whose elements are comprised of g_{ji} and h_{ji}, where $j = 1, 2, \ldots, N_s$. N_s represents the number of samples used in the Monte Carlo analysis and is consistent for all parameters. Next, a third matrix is constructed denoted $\mathbf{G_H}$ which is equal to $\mathbf{G}$ but with the i^{th} column replaced by the i^{th} column from $\mathbf{H}$. The normalized first order sensitivity index S_i for each input parameter is numerically estimated by [11]:

$$S_i = \frac{V_i}{V} = \frac{\frac{1}{N_s}\sum_{j=1}^{N_s} f(\mathbf{H})_j \big(f(\mathbf{G_H}^{(i)})_j - f(\mathbf{G})_j\big)}{\frac{1}{N_s}\sum_{j=1}^{N_s}\big(f(\mathbf{G})_j\big)^2 - \frac{1}{N_s}\sum_{j=1}^{N_s} f(\mathbf{G})_j f(\mathbf{H})_j}, \tag{26}$$

where $f(\cdot)_j$ is the model evaluation of the j^{th} row of each matrix. S_i estimates the independent contribution to the output variance of the wavemaker model for each input parameter i, but does not include higher order effects. The relationship between the first and higher order sensitivity indices for the parameters of a given model is based on the unconditional variance decomposition and is expressed as [12],

$$\sum_i S_i + \sum_i \sum_{q>i} S_{iq} + \sum_i \sum_{q>i} \sum_{r>q} S_{iqr} + \cdots + S_{123\ldots k} = 1, \tag{27}$$

where S_i is the first order index for each parameter i. The second order indices S_{iq} describe the joint effect of X_i and X_q where $[q \in \mathbb{Z} \mid i < q \leq k]$. For third order sensitivity indices, S_{iqr} represents the joint effect of X_i, X_q, and X_r where $[r \in \mathbb{Z} \mid i < q < r \leq k]$ and so forth for higher indices until $S_{123\ldots k}$, which represents the sensitivity index due to joint effect of all parameters. Therefore, to account for all interactions due to k input factors, a total of $2^k - 1$ sensitivity indices are required. For a model with a large number of input parameters, the number of required indices can become computationally prohibitive. Therefore, total effect sensitivity indices S_{Ti} [13] are calculated to determine the contributions of all terms in the variance decomposition which include X_i. The total effect sensitivity index S_{Ti} can be estimated by [11], [14]:

$$S_{Ti} = \frac{V_{Ti}}{V} = \frac{\frac{1}{2N_s}\sum_{j=1}^{N_s}\Big(f(\mathbf{G})_j - f(\mathbf{G_H}^{(i)})_j\Big)^2}{\frac{1}{N_s}\sum_{j=1}^{N_s}\big(f(\mathbf{G})_j\big)^2 - \frac{1}{N_s}\sum_{j=1}^{N_s} f(\mathbf{G})_j f(\mathbf{H})_j}. \tag{28}$$

By using the approach of total effect sensitivity S_{Ti}, only $2k$ indices are required for the GSA.

The uncertainty for the estimation of each sensitivity index can be determined by calculating its respective confidence interval. In this paper, 95% confidence intervals on the first order variance V_i and total effect variance V_{Ti} have been calculated using a numerical method [12] based on the form of the numerators in (26) and (28). Since the solution presented in [12] is based on previous forms of the estimators for S_i and S_{Ti}, the uncertainty equations have been modified for the present study. Thus, the modified 95% confidence intervals for the first order δV_i and total effect δV_{Ti} variances are given by,

$$\delta V_i = \frac{1.96}{\sqrt{N_s}}\Bigg(\frac{1}{N_s}\sum_{j=1}^{N_s}\Big[f(\mathbf{H})_j\big(f(\mathbf{G_H}^{(i)})_j - f(\mathbf{G})_j\big)\Big]^2 - \Big[\frac{1}{N_s}\sum_{j=1}^{N_s} f(\mathbf{H})_j\big(f(\mathbf{G_H}^{(i)})_j - f(\mathbf{G})_j\big)\Big]^2\Bigg)^{1/2}, \tag{29}$$

$$\delta V_{Ti} = \frac{1.96}{\sqrt{N_s}}\Bigg(\frac{1}{2N_s}\sum_{j=1}^{N_s}\Big[\Big(f(\mathbf{G})_j - f(\mathbf{G_H}^{(i)})_j\Big)^2\Big]^2 - \Big[\frac{1}{2N_s}\sum_{j=1}^{N_s}\Big(f(\mathbf{G})_j - f(\mathbf{G_H}^{(i)})_j\Big)^2\Big]^2\Bigg)^{1/2}. \tag{30}$$

Similarly, the confidence interval for the overall variance δV can be expressed as,

$$\delta V = \frac{1.96}{\sqrt{N_s}}\Bigg(\frac{1}{N_s}\sum_{j=1}^{N_s}\Big[\big(f(\mathbf{G})_j\big)^2\Big]^2 - \Big[\frac{1}{N_s}\sum_{j=1}^{N_s}\big(f(\mathbf{G})_j\big)^2\Big]^2\Bigg)^{1/2}. \tag{31}$$

Using error propagation, the uncertainty associated with the first order δS_i and total effect δS_{Ti} sensitivity indices therefore take the following forms,

$$\delta S_i = \left[\left(\frac{\delta V_i}{V}\right)^2 + \left(\frac{V_i \delta V}{V^2}\right)^2\right]^{1/2}, \tag{32}$$

$$\delta S_{Ti} = \left[\left(\frac{\delta V_{Ti}}{V}\right)^2 + \left(\frac{V_{Ti} \delta V}{V^2}\right)^2\right]^{1/2}. \tag{33}$$

A. Code Validation - Ishigami Function

The sensitivity indices of the Ishigami function have been analytically determined and thus, the performance of the GSA implemented in the current paper can be validated. The Ishigami function is given as,

$$f(X_i) = \sin(X_1) + b_1 \sin^2(X_2) + b_2 X_3^4 \sin(X_1), \tag{34}$$

where the parameter $b_1 = 7$ and b_2 is typically equal to either 0.1 or 0.05, depending on the literature [13], [16]. In the current paper, the fixed parameters have been set to $b_1 = 7$ and $b_2 = 0.05$. The uniform distribution of each input parameter ranges from $-\pi \leq x_i \leq \pi$. The Ishigami function is a benchmark for sensitivity analyses since all indices can be computed analytically and there is peculiar result in that $S_3 = 0$ yet S_{T3} cannot be neglected. The purpose of this example is to examine how the sensitivity estimators represented by (26) and (28) perform using the Monte Carlo computation compared to the exact analytical values. The total

variance V of the model and its partial variances can be obtained from the relations:

$$V = \frac{a^2}{8} + \frac{b\pi^4}{5} + \frac{b^2\pi^8}{18} + \frac{1}{2}, \tag{35}$$

$$V_1 = \frac{b\pi^4}{5} + \frac{b^2\pi^8}{50} + \frac{1}{2}, \tag{36}$$

$$V_2 = \frac{a^2}{8}, \tag{37}$$

$$V_3 = 0, \tag{38}$$

$$V_{12} = 0, \tag{39}$$

$$V_{13} = \frac{b^2\pi^8}{18} - \frac{b^2\pi^8}{50}, \tag{40}$$

$$V_{23} = 0, \tag{41}$$

$$V_{123} = 0. \tag{42}$$

Table I provides the results of the sensitivity analysis obtained through the Monte Carlo estimation using $N_s = 50000$, along with the exact values and the uncertainty associated with each estimated sensitivity index. The GSA for the Ishigami function reveals that S_2 has the largest individual influence on the output variance of the function. Since S_2 is approximately equal to S_{T2} in the estimation, there is no interaction between X_2 and the remaining parameters. On the other hand, the contrast between S_1 and S_{T1} signifies that X_1 does have some interaction with the other parameters. Since it has already been established that X_2 does not interact with the other parameters, X_1 must be interacting with X_3. Finally, the first order sensitivity index for X_3 is estimated as $-0.60\% \pm 0.63\%$. Theoretically, S_i and S_{Ti} must be greater than or equal to zero for the input parameters of any given model; however, since the sensitivity indices from a GSA are estimated using (26) and (28), negative values close to zero can occur. In the context of S_3, the negative value is simply a result of the approximation and its error places the estimation within range of its exact value of 0. $S_3 = 0$ indicates that X_3 has no influence on the output variance of the Ishigami function; however, since $S_{T3} > 0$, the parameter does interact with the other parameters in the model which agrees with previous results determined by examining X_1. The estimated values for the sensitivity indices are all in good agreement with the exact values determined analytically. Therefore, the authors' are confident that the methods used herein for the GSA of the wavemaker are valid.

Table I
ESTIMATED AND EXACT SENSITIVITY INDICES FOR THE ISHIGAMI MODEL WITH ERROR ON THE ESTIMATED INDICES.

Sensitivity Index		Exact [%]	Estimated [%]	Est. Error [%]
First Order	S_1	21.85	21.50	± 1.18
	S_2	68.69	69.36	± 2.21
	S_3	0.000	-00.60	± 0.63
Total Effect	S_{T1}	31.31	30.77	± 1.17
	S_{T2}	68.69	68.79	± 1.94
	S_{T3}	9.46	9.41	± 0.33

IV. GLOBAL SENSITIVITY ANALYSIS RESULTS

The following section presents the results of the variance-based global sensitivity analysis applied to the theoretical plunger-type wavemaker model. Plunger-type wavemakers are versatile as the wavemaker can be outfitted with different plunger sizes and shapes, depending on the desired wave profiles to be replicated. To account for various plunger sizes and current velocities, the GSA was conducted using a broad range for each input parameter's sample distribution in the Monte Carlo analysis. The uniform distribution for the six input parameters U, ω, β, d_μ, h, and M are outlined in Table II. The range of 50-400 for the number of boundary node points M is based on the range used by Wu [4], who examined the change in wavemaker transfer function a/s for M = 50, 100, 200, and 400. The analysis in [4] concluded that $M = 200$ was an appropriate choice to achieve accurate results with the wavemaker model. The remaining parameter distribution ranges represent values that are typically seen the laboratory setting, incorporating various geometries of both the wedge and water channel along with a broad range of wave frequencies ω and current velocities U. Using the sample distributions presented in Table II, the GSA was conducted on the new wavemaker model and the first order and total effect sensitivity indices were determined for each parameter along with the uncertainty on each estimate from (32) and (33).

Table II
UNIFORM PARAMETER DISTRIBUTIONS FOR PLUNGER-TYPE WAVEMAKER.

Parameter	Minimum	Maximum
U	0.0 [m/s]	2.5 [m/s]
ω	0.2π [rad/s]	10π [rad/s]
β	10 [Deg]	60 [Deg]
d_μ	0.01 [m]	0.30 [m]
h	0.30 [m]	2.00 [m]
M	50	400

The sensitivity indices and their associated numerical error for the general case are presented in Table III as percentages of the total output variance of the plunger-type wavemaker model. The frequency ω was determined by the GSA to have the highest impact on the output variance of the wavemaker model. The first order effect S_ω accounts for $28.47 \pm 0.81\%$ of the uncertainty in the model, while its total effect sensitivity index $S_{T\omega}$ is equal to $44.86 \pm 0.99\%$. The output variance of the wavemaker model is also greatly impacted by both the wedge's angle β and mean depth d_μ whose total effect sensitivity indices were $25.90 \pm 0.56\%$ and $24.21 \pm 0.55\%$, respectively. Comparatively, the height of the water h has a low impact on the output variance of the wavemaker. The first order sensitivity for h was estimated to be $S_h = 0.99 \pm 0.19\%$ and its total effect sensitivity $S_{Th} = 2.45 \pm 0.10\%$. However, the number of boundary node points M has the lowest sensitivity

Table III
PERCENT SENSITIVITY INDICES AND ERROR FOR THE PLUNGER-TYPE WAVEMAKER MODEL.

Parameter	$\mathbf{S_i}$ [%]	$\delta\mathbf{S_i}$ [%]	$\mathbf{S_{Ti}}$ [%]	$\delta\mathbf{S_{Ti}}$ [%]
U	0.74	$\pm$ 0.30	6.84	$\pm$ 0.16
ω	28.47	$\pm$ 0.81	44.86	$\pm$ 0.99
β	16.21	$\pm$ 0.61	25.90	$\pm$ 0.56
d_μ	16.90	$\pm$ 0.60	24.21	$\pm$ 0.55
h	0.99	$\pm$ 0.19	2.45	$\pm$ 0.10
M	0.02	$\pm$ 0.03	0.06	$\pm$ 0.00

indices where $S_M = 0.02 \pm 0.03\%$ and $S_{TM} = 0.06 \pm 0.00\%$. Therefore, M has the least amount of influence on the output variance of the wavemaker model.

For the presented parameter distributions, the current U independently accounts for $0.74 \pm 0.30\%$ of the output variance of the wavemaker model as given by the first order sensitivity index S_U. The total effect of the current, which includes the first order index and the interaction of U with the other parameters accounts for $6.84 \pm 0.16\%$ of the model's output variance. Despite the relatively low influence of U, experimental testing conducted using a wedge at Carleton University demonstrated an observable decrease in the wave amplitude to stroke amplitude ratio a/s for increasing current, the results of which are provided in Section I. From Table III, it can be concluded that the effect was mostly due to the total interaction of U with the other input parameters determined by $S_{TU} - S_U = 6.10 \pm 0.34\%$. Since the majority of the impact of the current velocity on the wavemaker amplitude ratio is due to the higher order effects in S_{TU}, inclusion of the water current as an uncertain input parameter in the wavemaker model is essential.

To demonstrate the influence of the current on the other wavemaker parameters, the GSA was rerun for three fixed values of U equal to 0, 1, and 2 m/s. Fig. 3 displays the first order sensitivity indices S_i of the input parameters ω, β, d_μ, h, and M for each fixed value of U. As the fixed value of the current is increased from 0 m/s to 1 m/s to 2 m/s, the first order sensitivity index for the frequency ω increased from 8.32% to 34.97% to 41.07%. The first order indices also increased for β and d_μ, where for U = 2 m/s, the influence of the parameters inverted resulting in the mean wedge depth having a larger influence on the model the wedge angle. The sensitivity of the wavemaker model to the water height h only has a small change relative to the previously mentioned parameters; however, there is still an observable difference in the sensitivity index as the current increases. Therefore, the interaction between the current U and water height h is relatively low compared to the frequency, mean wedge depth, and wedge angle. On the contrary, the first order sensitivity indices for the node points M remain constant for each current velocity at approximately zero. The total effect sensitivity indices S_{Ti} for ω, β, d_μ, h, and M are displayed in Fig. 4 for the three fixed values of U. For the three respective values

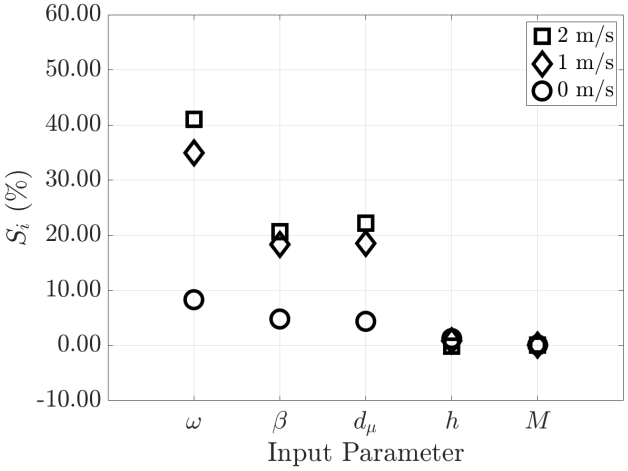

Figure 3. The first order sensitivity indices of the remaining input parameters when current is not included in the GSA.

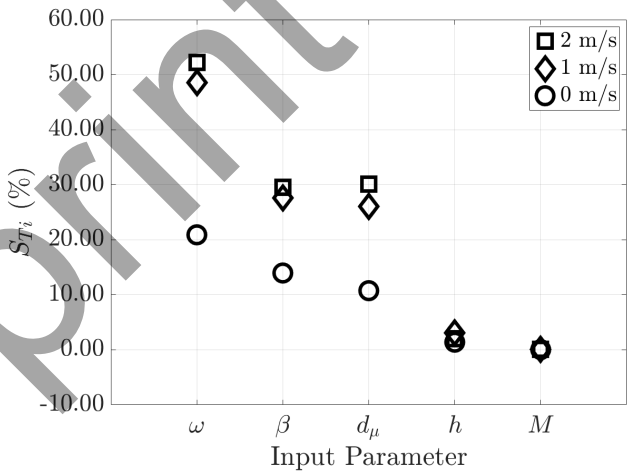

Figure 4. The total effect sensitivity indices of the remaining input parameters when current is not included in the GSA.

of U, the frequency ω had the largest deviation in the total effect sensitivity index $S_{T\omega}$ which increased from 20.90% to 48.53% to 52.19%. Similar trends as the first order sensitivity indices are also observed for the remaining parameters. By neglecting the effect of the current, the dependency of the wavemaker model on the remaining input parameters shifts with fluctuations in the current. As the current increases, the output model becomes more influenced by the wave frequency. Therefore, small errors in the measurement of the frequency could lead to large errors in the wave amplitude to stroke amplitude ratio a/s whereas for low current velocities, the uncertainty in the frequency measurement would not impact the output as much. Thus, even though the sensitivity indices for the current U in Table III are low compared to ω, β, and d_μ, the inclusion of current and its specific value must be considered in the wavemaker model.

In regards to the other input parameters, a notable observa-

tion is the sensitivity indices for the node points M. For the fixed current cases, the first order and total effect indices remained constant across all three current velocities with similar magnitudes to the results in Table III. As observed with S_3 of the Ishigami function in Section III-A, a sensitivity index close to zero indicates that the parameter has no influence on the uncertainty of the model. From the first order sensitivity index of M, it can be concluded that the number of node points does not individually impact the output variance of the wavemaker model. The total effect sensitivity index on the other hand indicates that M could have some interaction with the other input parameters. However, since $S_{TM} - S_M = 0.04 \pm 0.03\%$ is significantly lower relative to the influence of the other parameters, the number of node points M can be deemed a non-influential parameter and fixed to a deterministic value.

An additional observation is the low sensitivity indices for the water height h in Table III where $S_h = 0.99 \pm 0.19\%$ and $S_{Th} = 2.45 \pm 0.10\%$, and in Fig. 3 and Fig. 4 where the maximum indices are $S_h = 1.23 \pm 0.13\%$ and $S_{Th} = 3.07 \pm 0.11\%$. Through application of the boundary collocation method, Wu [4] concluded that the water height was a very important parameter in the plunger-type wavemaker model. However, the GSA of the model displayed that for a general distribution value of the input parameters, the water height had the lowest impact of the influential parameters on the wave amplitude to stroke amplitude ratio a/s of the wavemaker. Although the height of the water still needs to be measured and included in the model for hydrodynamic considerations, any uncertainty in the experimental measurement will not greatly impact the output of the theoretical model.

From a design standpoint, the GSA revealed that for the generation of waves by a plunger-type wavemaker, the uncertainty in the model will be governed by the uncertainty in the wave frequency. Therefore, for experimental testing, the uncertainty in the frequency measurement should be reduced as much as possible to minimize the uncertainty in the wave amplitude to stroke amplitude ratio a/s. Reducing the wave frequency uncertainty is especially critical when creating irregular wave spectra in a water channel, since the desired profile is dependent on a range of frequencies. The dimensions and positioning of the wedge should also be measured with reduced uncertainty as those parameters have the second and third highest influences on the output of the model. On the other hand, although the water height and current will influence the amplitude ratio, their lower sensitivity indices indicate that uncertainty in their measurements will not generate large uncertainties in the model. The specific sensitivity measurements of the GSA for wavemaker model are highly dependent on the uniform distribution range chosen for each input parameter. Although the general trend of the sensitivity indices would be similar to the results presented here, the analysis could also be applied to an experimental wavemaker for design considerations. In that case, the range for each parameter distribution would be established by either the uncertainty in the physical measurement of the parameter or a range of values at which to test the parameter. By applying the GSA to a specific experimental setup, the uncertainty in the transfer function between the wave amplitude and stroke amplitude can be improved. Thus, complex wave profiles can be accurately reproduced for marine engineering applications that require the inclusion of current such as ship motion and the launch and recovery of tow-bodies.

V. Conclusion

The model that relates the wave amplitude to the stroke amplitude for a plunger-type wavemaker in the presence of a uniform current was presented. In addition to the current U, the model requires five input parameters including the wave frequency, wedge angle, mean wedge depth, water height, the number of node points for the kinematic boundary condition. To investigate the effects of the current on the performance and design of the model, the method of variance-based global sensitivity analysis was introduced. The sensitivity analysis was applied to a broad distribution range for each parameter, providing results regarding the influence of all input parameters as well as their interactions with one another within the wavemaker model.

By determining the sensitivity of the wavemaker model to its input parameters, the theoretical design of the plunger-type wavemaker can be analysed for application to plungers in an experimental water channel. The GSA established that the number of node points required to define the kinematic boundary on the wavemaker is a non-influential parameter, such that uncertainty in the output of the wavemaker model will not be effected by changing its value. On the other hand, the analysis determined that the wave frequency has the largest influence on the output variance of the wavemaker model. Therefore, hydrodynamic applications dependent on plunger-type wavemakers should take caution when executing and determining the wave frequency for the model in order to achieve a desired wave profile. Compared to the wave frequency, the current has a low impact on the wavemaker model; however, its influence cannot be neglected. It was shown that by fixing the current in the wavemaker model to a set magnitude, the influence of each parameter changes as the value of the fixed current increases for both the first order and total effect sensitivity indices. Therefore, to accurately recreate a scaled ocean environment in a laboratory water channel, the uniform current must be measured and taken into consideration for the plunger-type wavemaker model.

Acknowledgment

The authors acknowledge the support of the Natural Sciences and Engineering Research Council of Canada (NSERC), [funding reference number RGPIN-2017-06967]. Cette recherche a été financée par le Conseil de recherches en sciences naturelles et en génie du Canada (CRSNG), [numéro de référence RGPIN-2017-06967]. Additionally, we would like to acknowledge Mitacs as support for the work was maintained through a Research Training Award (RTA) [reference number IT#19361], Kraken Robotic Systems Inc. for their support with

the hardware development, and Carleton University for the equipment infrastructure.

REFERENCES

[1] E.R. Chappell, "Theory and design of a wave generator for a short flume," MASc, University of British Columbia, Vancouver, British Columbia, 1969.

[2] T.H. Havelock F.R.S., "Forced surface-waves on water," *The London, Edinburgh, and Dublin Philosophical Magazine and Journal of Science*,vol. 8, no. 51, pp. 569-576, 1929.

[3] S. Wang, "Plunger-type wavemakers: theory and experiment," *Journal of Hydraulic Research*, vol. 12, no. 3, pp. 357-388, 1974.

[4] Y.-C. Wu, "Plunger-type wavemaker theory," *Journal of Hydraulic Research*, vol. 26, no. 4, pp. 483-491, 1988.

[5] D. Ellix and K. Arumugam, "An experimental study of waves genereated by an oscillating wedge," *Journal of Hydraulic Research*, vol. 22, no. 5, pp. 299-313, 1984.

[6] Y.-C. Wu, "Waves generated by a plunger-type wavemaker," *Journal of Hydraulic Research*, vol. 29, no. 6, pp. 851-860, 1991.

[7] J. McPhee, "Control, simulation, and testbed development for improving maritime launch and recovery operations," MASC, Carleton University, Ottawa, Ontario, 2019.

[8] I.M. Sobol', "Sensitivity analysis for non-linear mathematical models," *Mathematical Modelling and Computational Experiments*, vol. 1, no. 4, pp. 407-414, 1993.
Translated from Russian: I.M. Sobol', "Sensitivity estimates for nonlinear mathematical models," *Matematicheskoe Modelirovanie*, vol. 2, no. 1, pp. 112-118, 1990.

[9] R.G. Dean and R.A. Dalrymple,*Water Wave Mechanics for Engineers and Scientists*, Prentice-Hall, 1984.

[10] A. Saltelli, "Making best use of model evaluations to compute sensitivity indices," *Computer Physics Communications*,vol. 145, no. 2, pp. 280-297, 2002.

[11] A. Saltelli, P. Annoni, I. Azzini, F. Campolongo, M. Ratto, and S. Tarantola, "Variance based sensitivity analysis of model output. Design and estimator for the total sensitivity index," *Computer Physics Communications*, vol. 26, no. 6, pp. 723-730, 2010.

[12] A. Saltelli *et al.*, *Global Sensitivity Analysis: The Primer*, John Wiley & Sons, 2008.

[13] T. Homma and A. Saltelli, "Importance measures in global sensitivity analysis of model output," *Reliability Engineering and System Safety*, vol. 52, no. 1, pp. 1-17, 1996.

[14] M.J.W. Jansen, "Analysis of variance designs for model output," *Computer Physics Communications*, vol. 117, no. 1-2, pp. 35-43, 1999.

[15] T. Ishigami and T. Homma, "An importance quantification technique in uncertainty analysis for computer models," *Proceedings. First International Symposium on Uncertainty Modeling and Analysis*, University of Maryland, U.S.A., pp. 398-403, 1990.

[16] I.M. Sobol' and Yu.L. Levitan, "On the use of variance reducing multipliers in monte carlo computations of a global sensitivity index," *Computer Physics Communications*, vol. 117, no. 1-2, pp. 52-61, 1999.